Bulletin of the Seismological Society of America, Vol. 71, No. 3, pp. 731–745, June 1981

THE DENVER EARTHQUAKES OF 1967–1968

By Robert B. Herrmann, Sam-Kuen Park, and Chien-Ying Wang

ABSTRACT

A detailed study of the earthquakes associated with the Rocky Mountain Arsenal disposal well is presented. Long-period surface-wave studies are used together with *P*-wave first motions to show that the 10 April, 9 August, and 27 November 1967 earthquakes occurred at depths of 3 to 5 km and were characterized by normal faulting along a northwest striking fault plane. A joint hypocenter relocation of 103 microearthquakes of a data set of 279 recorded between 1967 and 1968 shows a hypocenter pattern striking N50°W, with most of the events located about 5 km northwest of the disposal well at depths between 3 to 8 km. A fault plane dipping southwest is tenuously suggested by those earthquakes with depths less than 5 km. Modeling of near-field seismoscope observations lend support to the focal mechanisms derived.

Introduction

The Denver earthquakes associated with the Rocky Mountain Arsenal disposal well during the 1960's are very important because they represent one of the first documented cases of the triggering of earthquakes due to high-pressure injection of fluids into host rock. The 3671.3-meter well into the top of the Precambrian was completed in 1961 and fluid injection commenced in early 1962 (Evans, 1966). Almost immediately, the relatively aseismic Denver area became seismically active. Following the suggestion of Evans (1966) of the possible causal relationship between the earthquakes and fluid injection, a number of geological and geophysical studies were initiated.

A detailed study of the seismicity and geology near the disposal well is contained in a report edited by Hollister and Weimer (1968). A study by Healy *et al.* (1968) reported on the results of a local seismograph array set up near the well together with the relationship of pumping to earthquake activity. The distribution of seismicity in 1966 indicated a narrow, shallow zone of seismicity striking northwest with the well near the center of epicenters. On the basis of a nodal plane of *P*-wave first motions crossing one of their L-shaped seismograph arrays, they inferred right-lateral strike-slip faulting on a fault plane striking northwest. Hoover and Dietrich (1969) tabulated hypocenter locations recorded by a U.S. Geological Survey (USGS) microearthquake array at the Arsenal during 1967 to 1968. These studies suggest that the seismicity migrated away from the well since the fluid injection began in 1962. Van Poollen and Hoover (1970) reviewed the history of the episode and discussed various causative mechanisms for the earthquakes as well as the results of a fluid removal experiment.

The best earthquake data were those collected by Hoover and Dietrich (1969). Using their local velocity model (Arsenal Model of Table 1), we have relocated the earthquakes they recorded using HYPO71 (Lee and Lahr, 1972). Figure 1 shows the locations of the arsenal well and the USGS seismograph locations, the epicenters, and projection of the epicenters onto vertical planes striking 40° and 130° with respect to north. The vertical line in the depth profiles indicates the well. It is obvious that few of the 289 hypocenters plotted are located at the well itself.

In spite of the many earthquakes recorded, little else is known about the sequence,

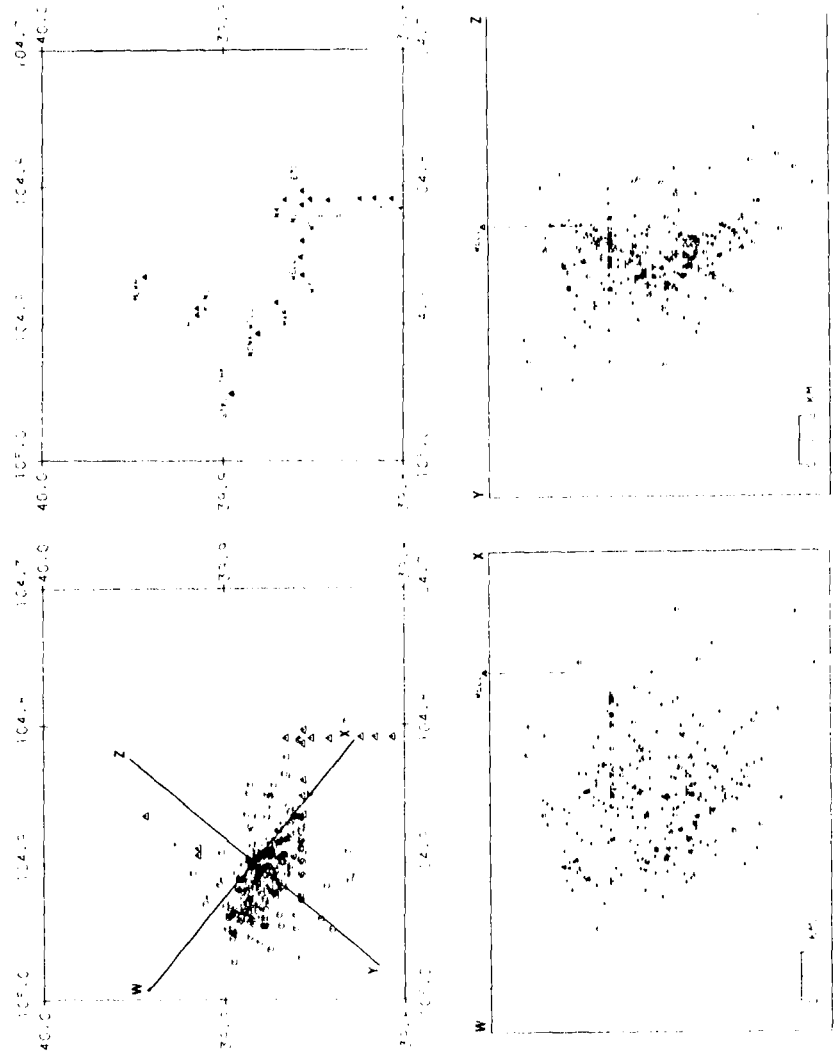

FIG. 1. Hypocenters determined from USGS array data. Epicenters and two vertical depth profiles are shown. The seismograph stations are indicated by triangles, with their names given on the base map. The position of the well is indicated on the epicenter maps and on the vertical depth projections.

primarily because they occurred almost 10 to 20 yr ago when the concept of portable microearthquake arrays was in its infancy. The focal depths and mechanisms of these earthquakes are poorly constrained. This paper seeks to examine other seismological data that can provide some information on these earthquakes.

Surface-Wave Studies

The 10 April, 9 August, and 27 November earthquakes of 1967 were large enough to generate long-period seismograms with a sufficiently large signal-to-noise ratio to warrant a detailed study. The focal mechanism and depth and seismic moment were obtained using the techniques described by Herrmann (1979). The Central United States earth model of Table 1 was used together with the eastern North American

TABLE 1
EARTH MODELS

H (km)	α (km/sec)	β (km/sec)	ρ (gm/cm^3)
	Central United States		
1	5.00	2.89	2.5
9	6.10	3.52	2.7
10	6.40	3.70	2.9
20	6.70	3.87	3.0
	8.15	4.70	3.4
	Colorado Plateau (Bucher and Smith, 1971)		
2.5	3.00	1.73	2.4
24.5	6.20	3.58	2.83
13.0	6.80	3.87	2.99
	7.80	4.25	8.33
	Arsenal		
0.38	2.17		
0.82	3.05		
1.15	3.22		
0.45	4.10		
0.15	4.60		
0.69	4.87		
1.06	5.80		
10.30	5.90		
	6.00		

anelastic attenuation coefficients of Herrmann and Mitchell (1975) for the inversion of the surface-wave spectral amplitude data. This choice is acceptable since the spectral amplitude data are relatively insensitive to earth model changes and since the models apply to most of the paths along which data were acquired.

Earthquake of 10 April 1967. This event was estimated to occur at 1900 UTC at 39.9°N, 104.8°W (ISC). We estimate $m_{bLg} = 4.3 \pm 0.2$ and $M_S = 4.2 \pm 0.2$, for the event using the relations of Nuttli (1973) and 13 short- and long-period WWSSN records. A total of 306 spectral amplitude-period pairs in the 6- to 40-sec period range from the 21 seismograph stations FFC, BLC, GWC, OTT, OGD, BLA, SLM, ATL, LUB, ALQ, TUC, DUG, LON, VIC, PHC, PNT, BOZ, FSJ, SES, YKC, and

CMC made up the vertical component Rayleigh-wave data set while 251 spectral amplitude-period pairs in the 6- to 40-sec period range from the same seismograph stations made up the Love-wave data set.

The focal mechanism solution which best fits the P-wave first motion and surface-wave data is shown in Figure 2. An equal area, lower hemisphere projection is used. Proceeding clockwise from north, the seismograph stations and their P-wave polarities are RKON(−), FKCO(−), ALQ(X), TUC(X), DEN(+), KNUT(+), GOL(+), DUG(+), LON(−), BOZ(+), PGBC(X), and SES(+). The P-wave takeoff angles used were 90° for distances of 30 to 100 km, 67° for distances of 160 to 185 km, 49° for 185 to 600 km, and 47° for 600 to 1650 km. At distances greater than 15° the table of Nuttli (1969) was used. The tension axis trends at 244° and plunges at 7°, and the pressure axis trends at 127° and plunges at 76°. A focal depth of 4 km and a seismic moment of 7.1×10^{22} dyne-cm were obtained. The correlation coefficients between the observed and predicted Rayleigh- and Love-wave spectral amplitudes were $r_R = 0.001$ and $r_L = 0.522$. The poor correlation coefficient r_R indicates first that the Rayleigh-wave data were of poor quality. Hence the focal mechanism is not

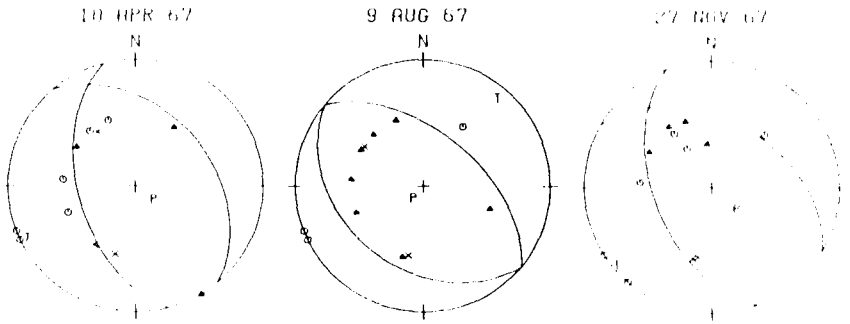

FIG. 2. Focal mechanisms of the 10 April, 9 August, and 27 November 1967 earthquakes. The nodal planes satisfy surface-wave spectral amplitude data as well as the P-wave first motion data. Circles, compressions; triangles, dilatations; X's uncertain arrivals of low amplitude. T and P are the intersections of the tension and pressure axes, respectively, with the lower hemisphere. An equal area lower hemisphere projection is used.

well constrained. A comparison of the anelastic attenuation corrected and theoretical radiation patterns is shown in Figures 3 and 4 for selected periods of the Love- and Rayleigh-wave data sets, respectively.

Given the sparse P-wave first motion data set, another test of the choice of compression and dilatation quadrants is a comparison of observed and theoretical surface-wave phases at selected stations. This is appropriate since the surface-wave amplitude spectra were used to specify the nodal planes while the P-wave first motion data were used to constrain the nodal planes somewhat, but more importantly the first motions were used to specify the compression and dilatation quadrants. ALQ at a distance of 572 km and DUG at a distance of 693 km were the closest seismograph stations that had on-scale long-period surface-wave recordings. The observed data were corrected for instrumental phase response as well as for the linear phase shift due to the difference between the origin time and the start of digitizing. An examination of the group velocities of the Love and Rayleigh waves indicated that the Colorado plateau earth model of Bucher and Smith (1971) would be a suitable regional model for the phase study. This earth model is given in Table 1.

Using that earth model, observed and theoretical phase spectra were compared at 17 periods between 16 and 32 sec. The average phase differences for the vertical component Rayleigh waves at ALQ and DUG were 0.805 ± 0.128 and 0.798 ± 0.122 circles, respectively. For the Love waves, the differences at ALQ and DUG were 0.943 ± 0.032 and 0.831 ± 0.120 circles, respectively. Since the phase differences given are in circles, 0.0 or 1.0 circles indicate a correct choice of the compressional and dilatational quadrants and 0.5 circles indicate an incorrect choice. Thus the

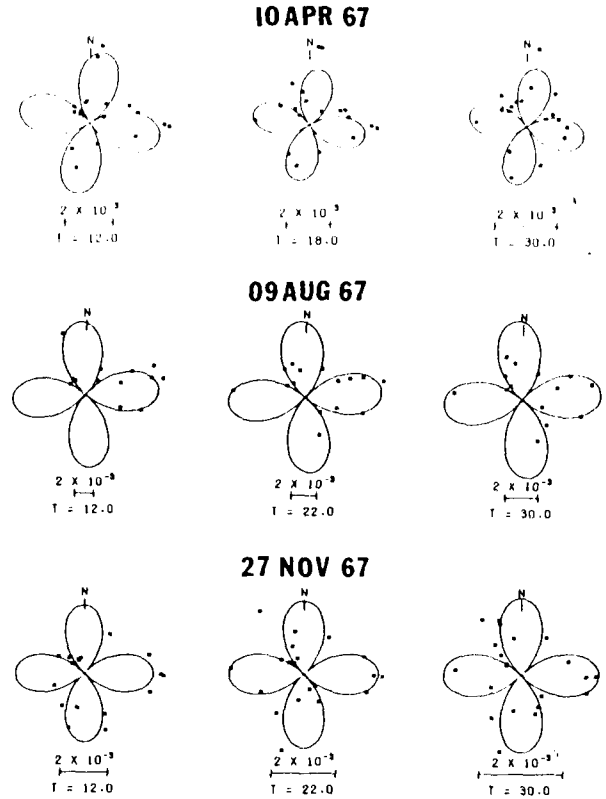

FIG. 3. Comparison between anelastic attenuation corrected observed and predicted Love-wave radiation patterns at selected periods, T, for the events studied. The scaling bars are spectral amplitudes in units cm-sec at a reference distance of 9° from the source.

choice of compression and dilatation quadrants is supported by the surface-wave phase data.

Earthquake of 9 August 1967. This earthquake occurred at 1325 UTC at 39.9°N and 104.7°W (ISC). Nuttli *et al.* (1979) assigned an $m_b = 4.9$ and an $M_S = 4.4$ to this event. A total of 279 spectral amplitude-period data pairs from the 18 seismograph stations BLC, FBC, GWC, SFA, OTT, SCB, AAM, OGD, ATL, OXF, DAL, ALQ, DUG, LON, BOZ, FSJ, EDM, and YKC in the 5- to 40-sec period range made up the vertical-component Rayleigh-wave spectral amplitude data set. The Love-wave

spectral amplitude data set was composed of 217 spectral amplitude-period data points in the 6- to 40-sec period range from the 15 seismograph stations FBC, SFA, OTT, SCB, OGD, ATL, OXF, DAL, LUB, DUG, LON, BOZ, FSJ, EDM, and YKC.

The focal mechanism which best fits the *P*-wave first motion and surface-wave data is shown in Figure 2. The tension axis trends at 40° and plunges at 10° while the pressure axis trends at 220° and plunges at 80°. A focal depth of 3 km and a seismic moment of 2.1×10^{23} dyne-cm were obtained. The seismograph stations and their *P*-wave first motions, clockwise from north, are RKON(+), OXF(−),

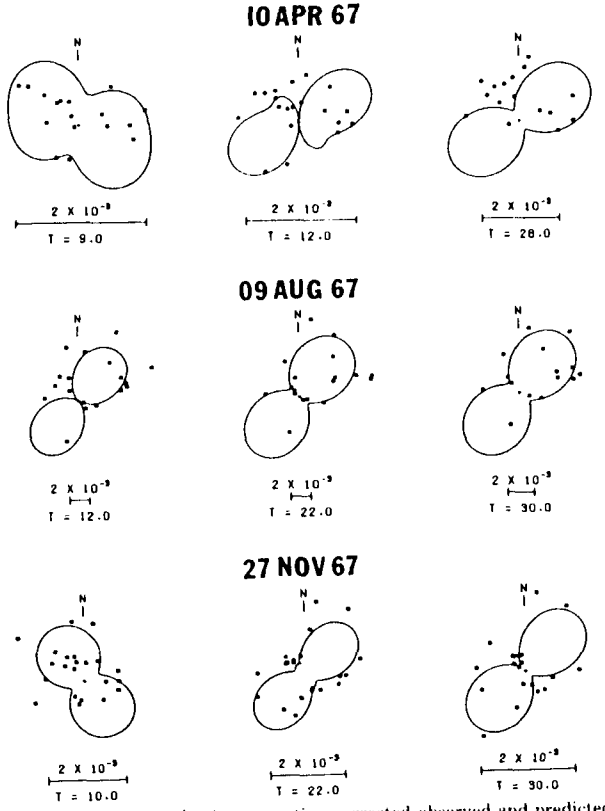

FIG. 4. Comparison between anelastic attenuation corrected observed and predicted Rayleigh-wave radiation patterns at selected periods for the events studied. The scaling bars are spectral amplitudes in cm-sec at a reference distance of 9° from the source.

LCNM(×), ALQ(−), DEN(+), KNUT(−), GOL(+), DUG(−), HLID(−), LON(×), PNT(−), and SES(−). The correlation coefficients between the observed and predicted Rayleigh- and Love-wave spectral amplitudes are $r_R = 0.692$ and $r_L = 0.697$, respectively. A comparison of the observed and predicted radiation patterns for selected periods of the Love- and Rayleigh-wave data sets is made in Figures 3 and 4.

For the focal mechanism given in Figure 2 for this earthquake, the average differences in circles between observed and theoretical phase spectra were 0.880 ± 0.071 and 0.109 ± 0.067 for the vertical component Rayleigh wave at ALQ and DUG, respectively, and 0.143 ± 0.040 for the Love wave at DUG. These support the normal fault, focal mechanism solution.

Earthquake of 27 November 1967. This event occurred at 0509 UTC at 40.0°N, 104.7°W (ISC). Nuttli *et al.* (1979) estimated an $m_b = 4.6$ and an $M_S = 3.8$ for this earthquake. The 23 seismograph stations FFC, BLC, RKON, WES, BLA, FLO, ATL, DAL, JCT, LUB, LCNM, ALQ, TUC, GSC, DUG, LON, PHWA, PNT, BOZ, PGBC, SES, HVMA, and YKC yielded 436 Rayleigh-wave and 435 Love-wave spectral amplitude-period observations in the same period range.

The resultant focal mechanism is shown in Figure 2. The tension axis trends at 230° and plunges at 4° while the pressure axis trends at 131° and plunges at 69°. A focal depth of 5 km and a seismic moment of 7.2×10^{22} dyne-cm were obtained. The *P*-wave first motion data are, clockwise from north, WNSD(+), LCNM(×), ALQ(×), DEN(+), GOL(+), DUG(+), HLID(−), TLWY(−), PGBC(+), WHYK(+), HVMA(−), and NPNT(−). The Rayleigh- and Love-wave correlation coefficients between the observed and predicted data were $r_R = 0.566$ and $r_L = 0.603$. Radiation pattern plots at selected periods are shown in Figure 3. For the focal mechanism derived, the differences in circles between observed and theoretical phase spectra were 0.899 ± 0.079 and 0.137 ± 0.035 for the vertical component Rayleigh wave at ALQ and DUG, respectively, and 0.118 ± 0.044 and 0.066 ± 0.035 for the Love wave at ALQ and DUG, respectively. These results support the choice of the compressional and dilatational quadrants.

The focal mechanism solutions of the 9 August and 27 November are very good and would be quality A solutions of Herrmann (1979). The 10 April solution is not very good. Because of background noise due to a large teleseism some hours before as well as low-spectral amplitudes due to the focal mechanism and depth, the fit between the observed and predicted Rayleigh-wave spectral amplitude data was marginal. In fact the Rayleigh-wave data are more consistent with a normal fault striking northeast rather than northwest. The accepted northwest solution fits the Love wave data as well and is also in agreement with the focal mechanisms of the other two earthquakes studied. The 10 April earthquake would be rated quality C.

Hypocenter Relocation

Hoover and Dietrich (1969) reported on the operation of an array of seismographs located near the disposal well. The locations of the stations are shown in Figure 1. Through the efforts of Dr. Hoover, punched data cards for 289 earthquakes recorded in the time period 1967 to early 1969 were obtained. The array operation was not continuous. No data from the array were available for the large 10 April, 9 August, and 27 November 1967 earthquakes. Thus a detailed study of their aftershocks with the goal of understanding the rupture process was not possible. However, the spatial relationship of these individual events to the disposal well was of interest.

This large earthquake data set encouraged the use of a joint hypocenter relocation technique (Douglas, 1967). The object is to simultaneously relocate all earthquakes, determining their hypocenters and origin times, and to obtain the station corrections and/or refined earth model. Normally this would not be feasible since a 1174×1174 matrix inverse (4×289 hypocenter parameters and 18 station corrections) would have to be calculated. However, a matrix partitioning technique outlined in the Appendix was used to solve the problem in such a way that the largest matrix inverted is only 18×18. Care must be taken in choosing the earthquakes used for

ocation since poorly constrained earthquakes will contaminate the location of the ıer earthquakes which are all interrelated through the station corrections.

Since this study was the first experience with joint hypocenter relocation techques by the authors, a number of decisions were made. First, a subset of 106 rthquakes, recorded by at least eight stations including one northwest of the well, ıs used. This requirement was established by trial and error in order to reduce the andard errors of the resulting epicenters and station corrections. Because of the mplexity of the joint hypocenter relocations equations (A1), it is difficult to sualize the interrelation between hypocenter and station correction adjustments. ı order to stabilize the problem either one hypocenter or one station correction ıust be fixed. A completely unconstrained solution is not possible since a systematic ıange in station corrections would be accounted for by a similar change in origin mes, e.g., increasing station corrections by 1.0 sec would force all origin times to be .0 sec earlier. Thus, a hypocenter or station correction constraint is required.

Since no one earthquake was better than any other, we decided to set the station orrection at W3 equal to zero. As the reviewer, Dr. James Dewey, pointed out, this onstraint affects only origin times and station corrections, but this does not affect he hypocenters which are free to move. This inversion thus uses the minimal ıumber of side constraints. The fact that the inversion was stable was due to a wide ange of ray paths available. If the source zone had been very localized, an *a priori* ıssumption of the location of one event would have been required. The simplicity ɔf just fixing one station correction may not be valid unless the station corrections ɔbtained actually reflect near-surface travel-time anomalies.

The results of the relocation are shown in Figure 5. From *top* to *bottom*, this figure shows the epicenter locations and projections of the epicenters on planes striking N40°E and N130°E. The *left column* presents the data set chosen for relocation, while the *right column* shows the results of the relocation. The relocated earthquakes cluster together better and have been moved to shallower depths. As mentioned by Hoover and Dietrich (1969) the seismic activity during this time period was not at the disposal well. As a matter of fact, almost all of the relocated hypocenters are more than 3 km from the base of the well.

It is disconcerting that a definite fault plane is not apparent after all the relocation effort. The surface-wave studies indicate that the fault plane should strike in the direction of seismicity and dip either to the northeast or southwest. A tenuous argument can be made in favor of the southwest dipping fault plane. There seems to be a different spatial relationship between those earthquakes occurring above and below 5 km in depth, with the deeper ones occurring nearer to the well. Looking in the direction of strike, the shallower earthquakes do seem to exhibit a southwestward dip. Unfortunately, we cannot be more precise.

Near-Field Studies

Twenty-five Wilmot seismoscopes were installed near the disposal well in 1966 in order to collect strong motion data (Hollister and Weimer, 1968). Seismoscope records are available from the 10 April and 9 August earthquakes. The numbered circles in Figures 6 and 7 are reproductions of the seismoscope traces due to the 10 April and 9 August earthquakes, respectively. The locations of the earthquakes with respect to the seismoscopes is given by the + sign (Hollister and Weimer, 1968).

Given this interesting data set, we were curious to see if we could model the observations. This was not an easy task since any errors in the focal mechanism and depth, source location, or earth model would affect the particle motion a great deal.

Because of this only the simplest model was used to synthesize the ground motions, that of a buried point source in a half-space. A Cagniard-de Hoop program (Johnson, 1974) was used to generate ground motion time histories at the free surface for an

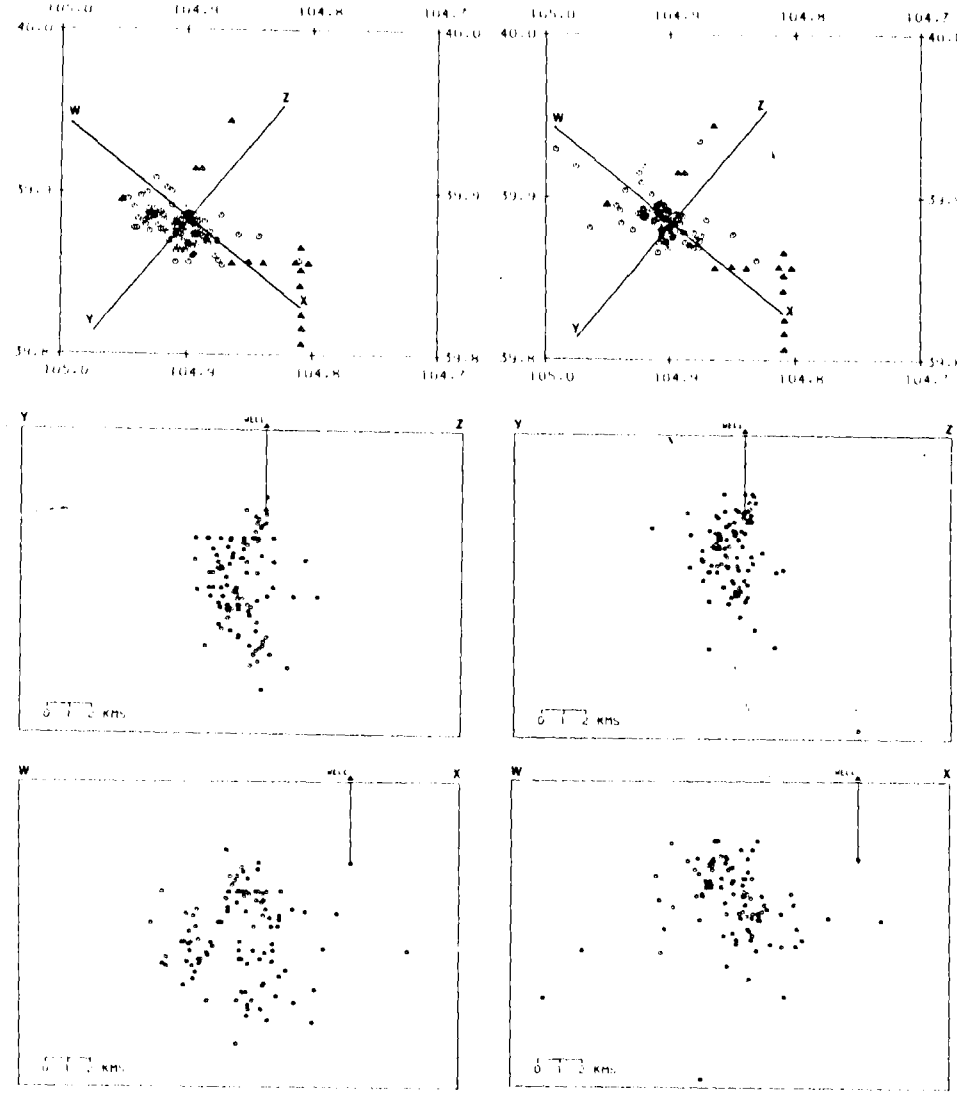

Fig. 5. The *left column* is the data set selected for joint hypocenter determination while the *right column* shows the relocated events. In each case the epicenters and two vertical depth profiles are shown. The well and seismographs stations, triangles, are indicated for reference. There is no vertical exaggeration.

earth model with compressional velocity of 6.0 km/sec, shear velocity of 3.45 km/sec, and density of 2.7 gm/cm^3. The horizontal components of the ground motions were passed through a single degree of freedom oscillator with $T_n = 0.78$ sec and η

= 10 per cent (Hudson and Cloud, 1967) to synthesize seismoscope traces. The source time function used was the parabolic pulse of Herrmann (1978) defined as

$$2Ts(t) = \begin{cases} 0 & t \leqq 0 \\ 0.5(t/T)^2 & 0 \leqq t \leqq T \\ -0.5(t/T)^2 + 2(t/T) - 1 & T \leqq t \leqq 3T \\ 0.5(t/T)^2 - 4(t/T) + 8 & 3T \leqq 5 \leqq 4T \\ 0 & t \geqq 4T. \end{cases}$$

This source pulse represents the velocity time history of the rupture.

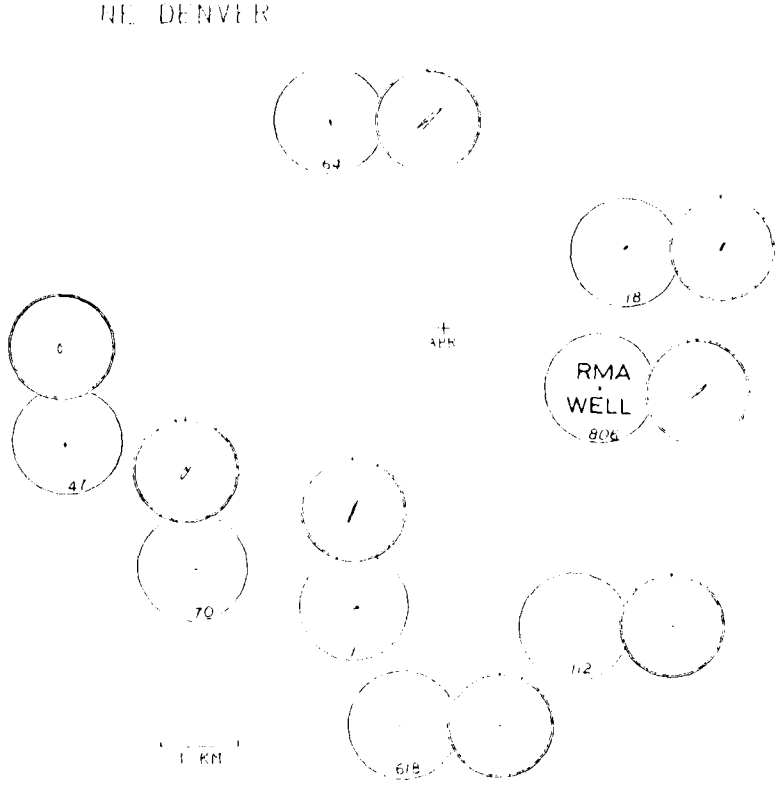

FIG. 6. A comparison between the observed and predicted seismoscope records for the 10 April 1967 earthquake. The numbered, singly circled plots are the observed data while the doubly encircled plots are the predicted data. All plots are scaled such that the diameter of each circle represents 6 cm on the original trace. The centers of the double circles indicate the actual locations of the seismoscope and the + symbol indicates the earthquake location given by Hollister and Weimer (1968).

Using the results of the surface-wave study and the locations of the 10 April and 9 August earthquakes given by Hollister and Weimer (1968) as a starting point, many synthetic seismoscope traces were generated for different values of T, focal depth and mechanism, seismic moment, and event location. The Hollister and Weimer (1968) locations provided the best fit. A good fit for the 10 April earthquake data was obtained using $T = 0.24$ sec, a source depth of 4 km, a seismic moment of 7.1×10^{22} dyne-cm, and a focal mechanism characterized by a strike of 140°, a dip

of 55°, and a slip of 80°. The predicted and observed traces are compared in Figure 6. The overall fit of shapes and amplitudes is quite good. Using the same focal depth and T values, a seismic moment of 2.1×10^{23} dyne-cm and a focal mechanism characterized by a strike of 135°, a dip of 55°, and a slip of 85° yielded the best fit to the data of the 9 August earthquake. The observed and predicted traces are given in Figure 7.

The agreement between the observed and predicted traces is surprisingly good,

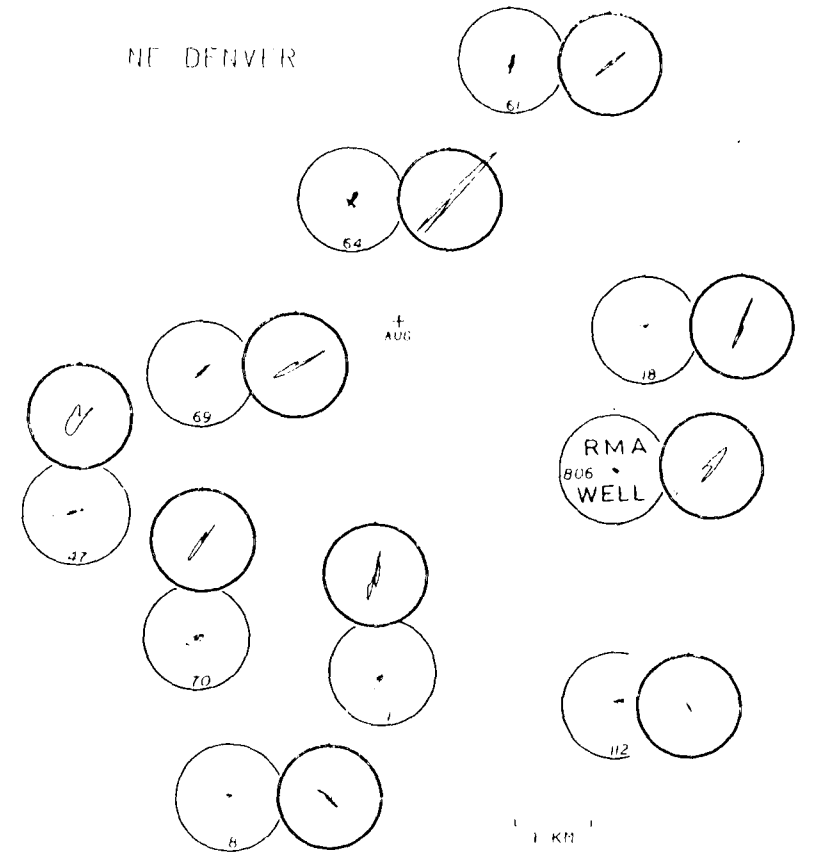

FIG. 7. A comparison between the observed and predicted seismoscope records for the 9 August 1967 earthquake. See Figure 6 for a description of the figure.

indicating the appropriateness of the source parameters. The focal mechanisms used are just slightly different than those obtained from the surface-wave analysis. The seismoscope simulation is really only a simplified test. Even though it is possible to generate time histories for a more realistic-layered earth structure, the unknowns in structure and the earthquake process did not warrant the additional effort. On the other hand, this exercise reinforces the surface-wave conclusions concerning the source depth and focal mechanism, and provides some constraints on the duration of the faulting process. This exercise also places some confidence in the Hollister

ıd Weimer (1968) locations, since data do not exist for the inclusion of these large ents into the joint hypocenter determination.

Conclusions

This detailed study of the three large Rocky Mountain Arsenal earthquakes of 967 has yielded new information on the seismic moment and focal mechanisms of hese earthquakes. The surface wave and *P*-wave first motion support northwest-triking normal faulting. Microearthquake data and simulation of seismoscope traces end support to this conclusion. The seismic moment of the 9 August earthquake nakes it one of the largest earthquakes east of the Continental Divide in the last 20 ır (Herrmann, 1979). Even though this study has not dealt with the relationship of he earthquakes to the disposal well, it is hoped that these results lead to a better nderstanding of the causative process of these earthquakes.

From a scientific point of view, it is unfortunate that these earthquakes occurred so long ago. The microearthquake data fortunately were still intact. They could easily have been lost. The sophistication of seismic instrumentation has improved substantially. Looking back, this earthquake sequence could have told us much more about the physics of an earthquake, in general, given modern instrumentation.

Acknowledgments

The efforts of Dr. Donald Hoover, U.S. Geological Survey, Denver, in locating the microearthquake data is gratefully acknowledged. This work was sponsored in part by the Department of the Interior, U.S. Geological Survey, Contract 14-08-0001-16708 and by the U.S. Nuclear Regulatory Commission Contract NRC-04-76-282. Dr. James W. Dewey provided a very enlightening review.

References

Bucher, R. L. and R. B. Smith (1971). Crustal structure of the eastern Basin and Range province and in the northern Colorado Plateau from phase velocities of Rayleigh waves, in *The Structure and Physical Properties of the Earth's Crust*, *Geophys. Monogr. Ser.*, vol. 14, J. G. Heacock, Editor, American Geophysical Union, Washington, D.C., 59–70.

Douglas, A. (1967). Joint hypocentre determination, *Nature* **215,** 47–48.

Evans, D. M. (1966). The Denver area earthquakes and the Rocky Mountain disposal well, *The Mountain Geologist* **3,** 23–36.

Healy, J. H., W. W. Rubey, D. T. Griggs, and C. B. Raleigh (1968). The Denver earthquakes, *Science* **161,** 1301–1310.

Herrmann, R. B. (1978). A note on causality problems in the numerical solution of elastic wave propagation in cylindrical coordinate systems, *Bull. Seism. Soc. Am.* **68,** 117–123.

Herrmann, R. B. (1979). Surface wave focal mechanisms for eastern North American earthquakes with tectonic implications, *J. Geophys. Res.* **84,** 3543–3552.

Herrmann, R. B. and B. J. Mitchell (1975). Statistical analysis and interpretation of surface-wave anelastic attenuation data for the stable interior of North America, *Bull. Seism. Soc. Am.* **67,** 209–218.

Hohn, F. E. (1964). *Elementary Matrix Algebra*, Macmillan Company, New York, 395 pp.

Hollister, J. C. and R. J. Weimer (Editors) (1968). Geophysical and geological studies of the relationships between the Denver earthquakes and the Rocky Mountain Arsenal well, *Q. Colorado School of Mines* **63,** Golden, 251 pp.

Hoover, D. B. and J. A. Dietrich (1969). Seismic activity during the 1968 test pumping at the Rocky Mountain Arsenal disposal well, *Geol. Surv. Circ. 613*, Washington, 35 pp.

Hudson, D. E. and W. K. Cloud (1967). An analysis of seismoscope data from the Parkfield earthquake of June 27, 1966, *Bull. Seism. Soc. Am.* **57,** 1145–1159.

Johnson, L. R. (1974). Green's function for Lamb's problem, *Geophys. J.* **37,** 99–131.

Lee, W. H. K. and J. C. Lahr (1972). HYP071: a computer program for determining hypocenter, magnitude, and first motion patterns of local earthquakes, *U.S. Geol. Surv. Open-File Rept. 75-311*, 113 pp.

Nuttli, O. W. (1969). Tables of angles of incidence of P wave at focus, calculated from 1968 P Tables, *Earthquake Notes* **40,** 21–25.

Nuttli, O. W. (1973). Seismic wave attenuation and magnitude relations for eastern North America, *J. Geophys. Res.* **78,** 876–885.

Nuttli, O. W., G. A. Bollinger, and D. W. Griffiths (1979). On the relation between Modified Mercalli intensity and body-wave magnitude, *Bull. Seism. Soc. Am.* **69,** 893–909.

Spencer, C. and D. Gubbins (1980). Travel-time inversion for simultaneous earthquake location and velocity structure determination in laterally varying media, *Geophys. J.* **63,** 95–116.

van Poollen, H. K. and D. B. Hoover (1970). Waste disposal and earthquakes at the Rocky Mountain Arsenal, Derby, Colorado, *J. Petr. Tech.* **22,** 983–993.

Department of Earth and Atmospheric Sciences
Saint Louis University
P.O. Box 8099, Laclede Station
St. Louis, Missouri 63156

Manuscript received September 2, 1980

Appendix

As mentioned in the text, the application of joint hypocenter techniques to large numbers of earthquakes becomes difficult because of the large matrices which must be inverted. Without getting into the details of the joint hypocenter method, the normal equations to be solved are of the form

$$\begin{bmatrix} a_1 & 0 & \cdot & 0 & b_1 \\ 0 & a_2 & \cdot & 0 & b_2 \\ \cdot & \cdot & \cdot & \cdot & \cdot \\ 0 & 0 & \cdot & a_n & b_n \\ b_1^T & b_2^T & \cdot & b_n^T & c \end{bmatrix} \begin{bmatrix} x_1 \\ x_2 \\ \cdot \\ x_n \\ u \end{bmatrix} = \begin{bmatrix} y_1 \\ y_2 \\ \cdot \\ y_n \\ v \end{bmatrix} \tag{A1}$$

where the a_i is the usual (4×4) matrix of the single event location problem, y_i is a (4×1) matrix, x_i is a (4×1) matrix given the adjustments to the spatial coordinates and origin time, b_i is a $(4 \times M)$ matrix, c is an $(M \times M)$ matrix, v is $(M \times 1)$, and u is the $(M \times 1)$ matrix of adjustments to the station correction or earth model.

With the exception of the elements shown the large matrix of (A1) is very sparse. Because of this, a solution by matrix partitioning is suggested. The first row of (A1) can be written as

$$a_1 x_1 + b_1 u = y_1 \tag{A2}$$

or as

$$x_1 = a_1^{-1} y_1 - a_1^{-1} b_1 u.$$

Likewise,

$$x_2 = a_2^{-1} y_2 - a_2^{-1} b_2 u$$

through

$$x_n = a_n^{-1} y_n - a_n^{-1} b_n u.$$

Substituting these expressions for x_k into the last row of (A1), one obtains

$$[c - b_1^T a_1^{-1} b_1 - b_2^T a_2^{-1} b_2 - \cdots - b_n^T a_n^{-1} b_n]\, u = [v - b_1^T a_1^{-1} y_1 - b_2^T a_2^{-1} y_2 - \cdots - b_n^T a_n^{-1} b_n]. \tag{A3}$$

(A3) is a square matrix of dimensions $(M \times M)$. After solving (A3) for u, the u can be back-substituted into (A2) to obtain x_i, etc. If disk or other storage media are used, the maximum array required to be stored in the computer at any one time is $(M \times M)$.

The above method is very efficient in solving for the source parameter and station correction perturbations. In order to estimate the confidence on the latest perturbation, the inverse of the left-hand side of (A1) is required. While the desired elements of the variance-covariance matrix could be obtained by making the right side of (A1) the different columns of the identity matrix in succession, a matrix inversion by partitioning (Hohn, 1964) works very well.

Equation (A1) can be written as

$$\begin{bmatrix} A & B \\ B^T & c \end{bmatrix} \quad \begin{bmatrix} X \\ u \end{bmatrix} = \begin{bmatrix} Y \\ v \end{bmatrix} \tag{A4}$$

where A is the square matrix of the a_i's, $B = [b_1 b_2 \cdots b_n]^T$, and similarly for X and Y.

The first equation of (A4) can be manipulated to form

$$X = A^{-1}Y - A^{-1}Bu. \tag{A5}$$

Substituting this into the second equation, we get

$$[c - B^T A^{-1} B]u = [v - B^T A^{-1} Y]. \tag{A6}$$

Setting

$$D = A^{-1}B \quad \text{and}$$
$$E = c - B^T A^{-1} B = c - B^T D,$$

we have

$$u = (-DE^{-1})^T Y + E^{-1} v,$$

where we have used the fact that the original square matrix and hence E are symmetric. Back substituting,

$$X = [A^{-1} + DE^{-1}D^T]Y + [-DE^{-1}]v.$$

By examination, the inverse matrix for (A4) is

$$\begin{bmatrix} A^{-1} + DE^{-1}D^T & (-DE^{-1}) \\ (-DE^{-1})^T & E^{-1} \end{bmatrix}$$

which is symmetric.

Upon substituting the proper matrices from (A1) into (A4), we find that

$$\begin{aligned} E &= c - B^T A^{-1} B \\ &= [c - b_1{}^T a_1{}^{-1} b_1 - \cdots - b_n{}^T a_n{}^{-1} b_n]. \end{aligned} \tag{A7}$$

The right side is immediately recognized from (A3). Since the inverse of E is routinely computed in order to get the perturbations, the information on the variances for the station corrections is already available. Since, we are only interested in the (4×4) covariance matrix for each event and not in the covariance between events or between the event and the station corrections, it can be shown that the (4×4) covariance matrix for the first event is just

$$[a_1{}^{-1} + a_1{}^{-1} b_1 E^{-1} b_1{}^T a_1{}^{-1}]. \tag{A8}$$

A paper just published by Spencer and Gubbins (1980) presents a similar development but extends it simply and elegantly to include stochastic and generalized inverses. The difference between this presentation and theirs lies in the way (A2) and (A3) are written. Given adequate disk storage, there is no program size limitation to the maximum number of events that may be studied, there is only a disk storage limitation.